

THERMAL STABILITY OF TI NANOPARTICLES COATED BY Ni

¹Miroslav CIESLAR, ¹Lucia BAJTOŠOVÁ, ¹Nikoleta ŠTAFENOVÁ, ¹Elena CHOCHOLÁKOVÁ,
¹Jan HANUŠ, ²Jan FIKAR

¹Charles University, Faculty of Mathematics and Physics, Prague, Czech Republic, EU,

Miroslav.Cieslar@mff.cuni.cz, 96473937@o365.cuni.cz,

nikoleta.staffenova635@student.cuni.cz, ech4285@gmail.com, Jan.Hanus@mff.cuni.cz%20

²Czech Academy of Sciences, Institute of Physics of Materials, Brno, Czech Republic, EU, fikar@jpm.cz

<https://doi.org/10.37904/metal.2024.4907>

Abstract

Ti nanoparticles were deposited on a glass substrate by a gas aggregation source and coated with a thin layer of Ni under different deposition conditions. The resulting composite consists either of a mixture of TiO₂-covered Ti nanoparticles or core-shell Ti-Ni nanoparticles embedded in the Ni matrix. The thermal stability of the composite was studied during in-situ heating in the transmission electron microscope. Corresponding changes in the morphology of nanoparticles and the phase composition of the material were analyzed by energy-dispersive X-ray analysis and scanning (transmission) electron microscopy. The influence of the heating rate during the quasi-isochronal heating regime was tested. The coagulation of Ni in the Ti-Ni core-shell system was confirmed by molecular dynamics simulation.

Keywords: Nanoparticles, magnetron sputtering, Ti@Ni core-shell, in situ TEM annealing

1. INTRODUCTION

Self-propagating High-temperature Synthesis (SHS) is a relatively novel and straightforward method for producing advanced ceramics, composites, and intermetallic compounds [1, 2]. Porous TiNi alloys created via SHS exhibit promising potential in medical applications due to their superelasticity, shape-memory properties, excellent biocompatibility, high strength, shock resistance, and anti-wear/anticorrosion characteristics [3, 4]. Additionally, SHS has been effectively utilized for simultaneous net-shape production and joining, although understanding the joining process is still in its early stages [5]. The foundation of SHS lies in the ability of highly exothermic reactions to sustain themselves through a reaction (combustion) wave [6]. Despite their highly exothermic nature, these reactions require an external energy source to initiate. It can be achieved by heating one end of the sample with thermal radiation or laser energy. Another method, known as the "thermal explosion" technique, involves heating the entire sample to a temperature where the reaction spontaneously occurs [7].

SHS reactions have also been observed in Ni-Ti multilayer films [8], possessing a great potential as an external heat source in a wide area of applications, including joining [9, 10], ignitors [11], and intermetallic synthesis [12] on the nanoscale. A novel approach uses nanoparticles to achieve similar self-propagating reactions on a nanoscale. This concept is up-and-coming due to the ease of application of nanoparticles on various surfaces. Core-shell nanoparticles, especially those with a titanium (Ti) core and a nickel (Ni) shell, are of significant interest. This configuration ensures a stable Ni to Ti ratio while the Ni shell protects the Ti core from oxidation, preserving its reactive properties. However, several studies on bulk Ni-Ti systems show that preheating and rapid ignition temperature increases are necessary to start the combustion [13,14]. Low heating rates, on the other hand, limit the SHS and inhomogeneous structure with separated Ni and Ti forms.

This study investigates the thermal stability of Ti-Ni core-shell nanoparticles produced using a gas aggregation source. The thermal behavior of the composite was examined through slow in-situ heating within the transmission electron microscope (TEM), allowing for real-time observation of morphological and phase composition changes and identification of mechanisms controlling the separation of Ni and Ti. Experimental findings were completed with molecular dynamics (MD) simulations.

2. MATERIAL AND METHODS

DC magnetron sputtering with two planar magnetrons was used to prepare Ti@Ni core-shell nanoparticles and a mixture of Ni and Ti nanoparticles. The sputtering system consisted of a primary gas aggregation cluster source (GAS) for producing Ti nanoparticles (NPs) and a secondary chamber for coating them with a Ni film or production of Ni nanoparticles. Ar gas with 99.996% purity was used as the working gas with a pressure of 48 Pa in the Ti and 5.6 Pa in the Ni chamber, currents of 500 mA on the Ni and 400 mA on the Ti magnetron for the mixture preparation, and of 400 mA on the Ni and 150 mA on Ti magnetron for the core-shell particles. Further details about the experimental setup are available in the work by Hanus et al. [15]. The nanoparticles were deposited onto a glass substrate. The samples were prepared for TEM analysis by depositing the nanoparticles, suspended in methanol, onto a grid with a SiN support film. A Jeol 2200FS transmission electron microscope operated at 200 kV was employed in STEM mode, equipped with bright field (BF), high-angle annular dark field (HAADF), and secondary electrons (SEI) detectors and energy dispersive spectroscopy (EDS).

For MD simulations, the LAMMPS software [16] was used with a modified embedded atomic potential for aluminum [17] to describe the inter-atomic interactions. A pile of core-shell Ti@Ni nanoparticles was created by Atomsk [18], and the results were visualized by Ovito [19].

3. RESULTS

STEM BF and SEI detectors were used to characterize the mixture of Ni and Ti nanoparticles without the core-shell structure prepared by magnetron sputtering (**Figure 1a,b**). Ni nanoparticles are generally smaller than Ti ones. The core-shell structure can be clearly observed in the BF image on Ti nanoparticles. It is due to the oxidation of the particles. An amorphous TiO₂ shell is formed on the Ti nanoparticles due to the higher reactivity of Ti. The particles were annealed up to 850 °C with temperature step 50 K/10 min (**Figure 1 c, d**). The Ti particles with the shell kept their shape, while the sintering of smaller Ni nanoparticles without the shell can be observed.

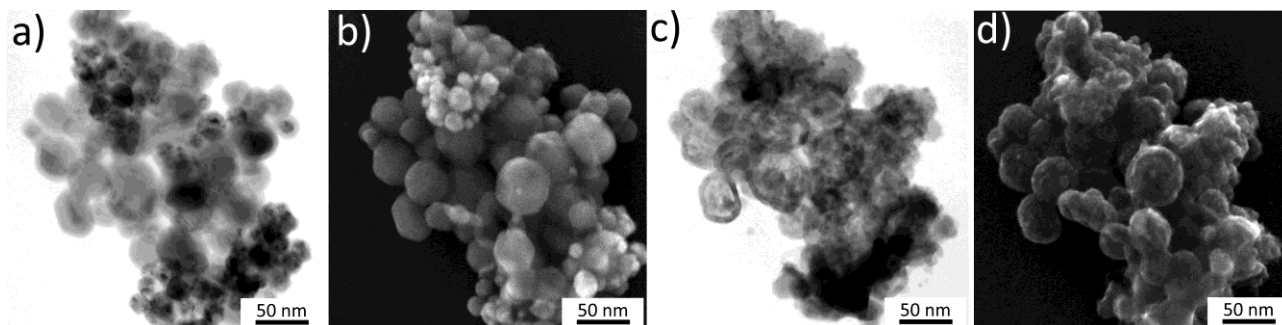


Figure 1 Mixture of Ni and Ti nanoparticles – STEM images: a,c) BF, b,d) SEI detector, a,b) RT, c,d) specimen annealed up to 850 °C

Further annealing up to 950 °C resulted in the formation of over 200 nm large particles (**Figure 2**). The chemical analysis of the annealed sample was performed after the cooling down to room temperature. Ti nanoparticles

did not grow significantly at this temperature. Ni and Ti parts remained separated, and no formation of binary Ni-Ti phase occurred.

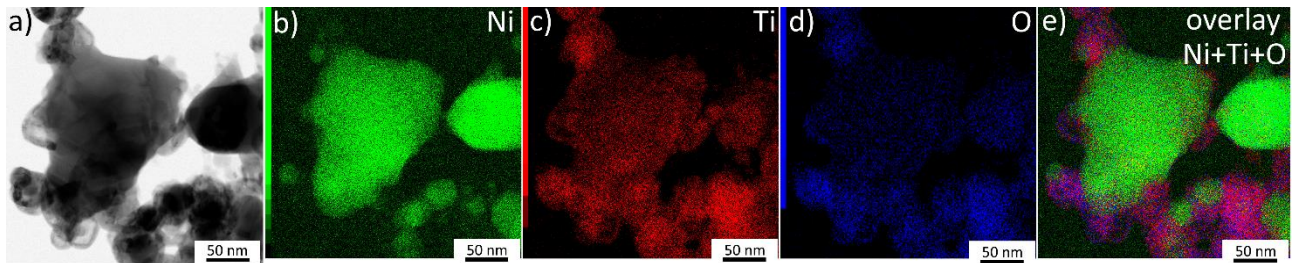


Figure 2 The mixture of Ni and Ti nanoparticles annealed up to 950 °C – a) STEM BF image, b-e) EDS analysis

The formation of core-shell nanoparticles with Ni shell and Ti core was achieved by adjusting the current on both magnetrons. This core-shell structure was confirmed by STEM and EDS analysis (**Figure 3**).

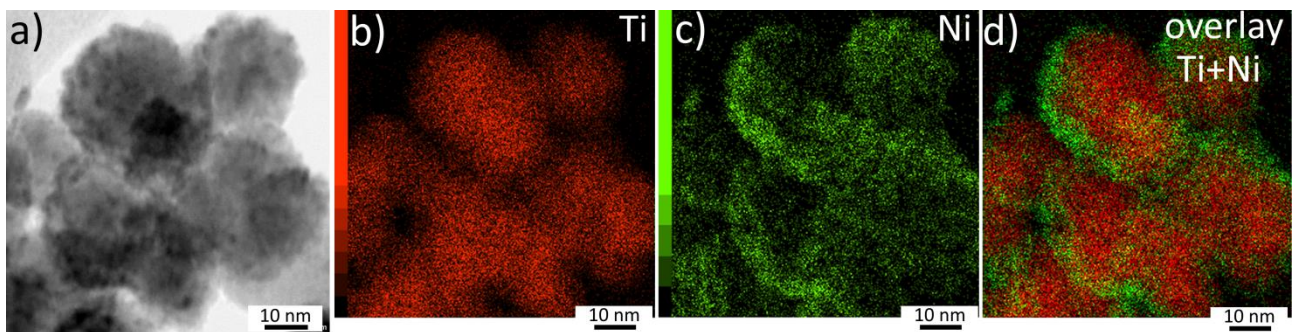


Figure 3 Ti@Ni core-shell nanoparticles: a) STEM BF, b-d) EDS maps

Similarly to the Ni and Ti nanoparticles mixture, Ti@Ni core-shell nanoparticles were annealed up to 900 °C (**Figure 4**). Again, sintering and formation of large particles can be observed at 700 °C. The sintering further continues with increasing temperature up to 900 °C. EDS maps (**Figure 5**) show that the largest particles contain only Ni. The initially core-shell nanoparticles lose their Ni shells, which sinter into new, above 100 nm large Ni particles. Meanwhile, the first signs of Ti cores sintering could be found.

The initial stages leading to the separation of both elements were simulated by molecular dynamics. A pile of four core-shell nanoparticles with Ni shell and Ti core diameter 3.6 nm was held at constant temperature. The simulations were performed at a temperature of 965 °C and pressure controlled by a Nose–Hoover thermostat and barostat as implemented in LAMMPS and with a one fs time step. Behavior corresponding to the experiment results can be observed (**Figure 6**), namely, the decrease of the pile surface caused by the surface diffusion of Ni. This process is finished at 250 ps, and only a sluggish interdiffusion of Ni and Ti can be observed at 1000 ps.

The timescale is sufficient for diffusion processes at low heating rates. Surface diffusion plays a significant role due to the high surface-to-volume ratio in nanoparticles and the higher diffusion coefficients for surface diffusion compared to bulk diffusion [20]. For nickel (Ni), the pre-exponential factor D_0 for calculating the diffusion coefficient for volume diffusion is $1.9 \times 10^{-4} \text{ m}^2/\text{s}$, with an activation energy of 280 kJ/mol [21]. Different values have been reported for the surface diffusion of Ni, with the pre-exponential factor ranging between 10^{-7} and $10^{-2} \text{ m}^2/\text{s}$ and the activation energy varying between 70 and 190 kJ/mol [21]. For titanium (Ti), similar values have been measured for volume diffusion, with a pre-exponential factor of $10^{-4} \text{ m}^2/\text{s}$ and an

activation energy of 276 kJ/mol [22]. Information on surface diffusion of Ti is limited. However, grain boundary (GB) diffusion has been measured in thin nanocrystalline films, with a pre-exponential factor

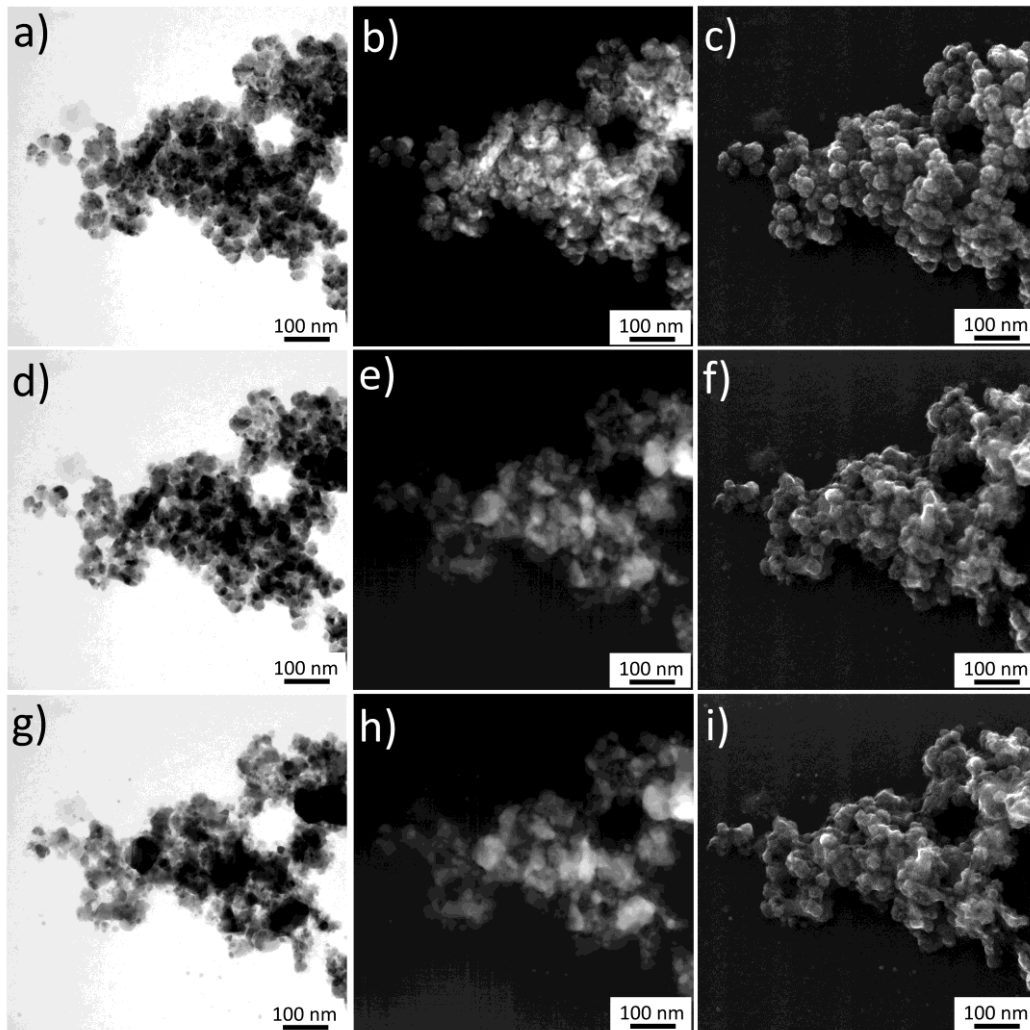


Figure 4 Annealing of Ti@Ni core-shell nanoparticles: a-c) RT, d-f) 700 °C, g-i) 900 °C, a,d,g) STEM BF, b,e,h) STEM HAADF, c, f, i) STEM SEI

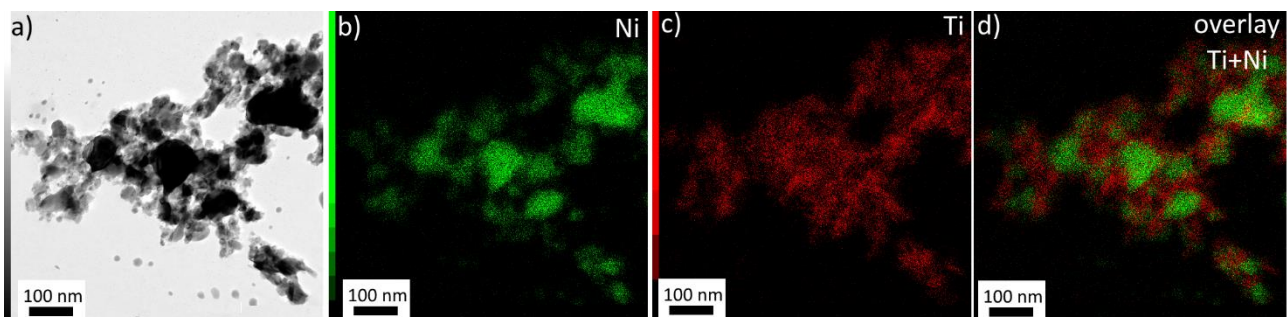


Figure 5 Annealed Ti@Ni core-shell nanoparticles after cooling to room temperature: a) STEM BF, b-d) EDS maps

of 7×10^{-12} m²/s and activation energy of 75 kJ/mol [23], values leading to significantly lower surface diffusion rates than in Ni [21].

During the annealing process, the sintering of Ni nanoparticles via surface diffusion occurs as they seek to minimize surface energy, resulting in the formation of larger Ni nanoparticles [20]. This aggregation leads to the separation of Ni and Ti, thereby preventing the occurrence of the SHS reaction.

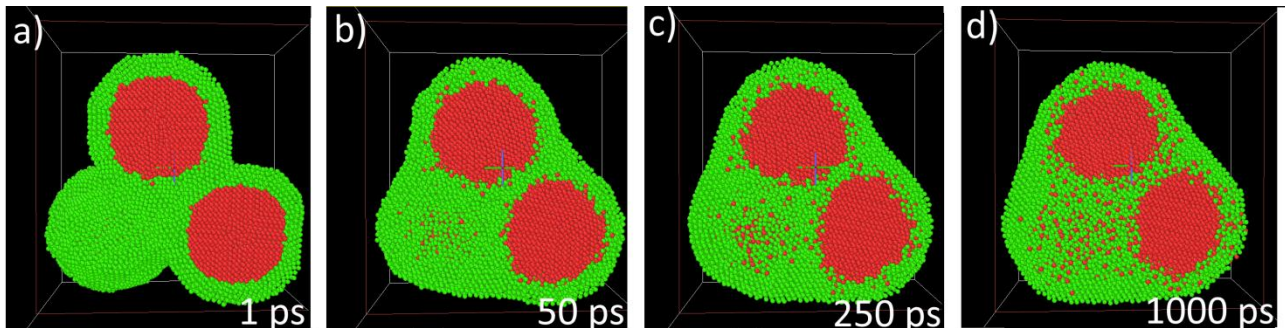


Figure 6 MD simulation of annealing of Ti@Ni core-shell nanoparticles, red: Ti, green: Ni, a) 1 ps, b) 50 ps, c) 250 ps, d) 1000 ps of simulation time

4. CONCLUSION

This study demonstrated the thermal behavior of Ti-Ni core-shell and mixed Ni and Ti nanoparticles prepared via magnetron sputtering. In-situ TEM heating revealed that Ni nanoparticles in the mixture and Ni shells in the core-shell particles tend to sinter and form larger particles at elevated temperatures. The process is driven by surface diffusion and surface energy minimalization. In contrast, Ti nanoparticles and cores retained their structure up to higher temperatures. It leads to the separation of Ni and Ti and prevents SHS reactions. Molecular dynamics simulations supported these observations, showing the diffusion and sintering behavior of the Ni shell. These findings emphasize the importance of controlling heating rates to promote desired reactions in advanced material applications.

ACKNOWLEDGEMENTS

This research was funded by the Czech Science Foundation, grant number 22-22572S.

REFERENCES

- [1] VIDYUK, T.M. et al. Synthesis of ceramic and composite materials using a combination of self-propagating high-temperature synthesis and spark plasma sintering (Review). *Combustion, Explosion, and Shock Waves*. 2021, vol. 57, pp. 385–397. ISSN 0010-5082. DOI: <https://doi.org/10.1134/S0010508221040018>.
- [2] OVCHARENKO, V.E. et al. High-temperature synthesis of Ni₃Al intermetallic compound under pressure. *Izvestiya Vysshikh Uchebnykh Zavedenii. Tsvetnaya Metallurgiya*, 2007, no. 4, pp. 63–69.
- [3] YASENCHUK, Y. et al. Biocompatibility and clinical application of porous TiNi alloys made by self-propagating high-temperature synthesis (SHS). *Materials*. 2019, vol. 12, no. 15, article 2405. ISSN 1996-1944. DOI: <https://doi.org/10.3390/ma12152405>.
- [4] ZHANG, L. et al. Superelastic behaviors of biomedical porous NiTi alloy with high porosity and large pore size prepared by spark plasma sintering. *Journal of Alloys and Compounds*. 2015, vol. 644, pp. 513-522. ISSN 0925-8388. DOI: <https://doi.org/10.1016/j.jallcom.2015.05.063>.
- [5] ORLING, T.T., MESSLER, R.W. Self-propagating high-temperature synthesis as a process for joining materials. *Welding Journal*. 1996, vol. 75.
- [6] MERZHANOV, A.G. *Self-Propagating High-Temperature Synthesis*. In: Physical Chemistry. Contemporary Problems. Moscow: Khimiya, 1983, pp. 6–45.

- [7] MUNIR, Z.A., ANSELMI-TAMBURINI, U. Self-propagating exothermic reactions: The synthesis of high-temperature materials by combustion. *Materials Science Reports*. 1989, vol. 3, issues 7–8, pp. 277-365. ISSN 0920-2307. DOI: [https://doi.org/10.1016/0920-2307\(89\)90001-7](https://doi.org/10.1016/0920-2307(89)90001-7).
- [8] SEN, S., LAKE, M., SCHAAF, P. Al-based binary reactive multilayer films: Large area freestanding film synthesis and self-propagating reaction analysis. *Applied Surface Science*. 2019, vol. 474, pp. 243-249. ISSN 0169-4332. DOI: <https://doi.org/10.1016/j.apsusc.2018.02.207>.
- [9] SURYANARAYANA, C., MOORE, J.J., RADTKE, R.P. Novel methods of brazing dissimilar materials. *Advanced Materials and Processes*. 2001, vol. 159, p. 29.
- [10] QIU, X., WANG, J. Bonding silicon wafers with reactive multilayer foils. *Sensors and Actuators, A: Physical*. 2008, vol. 141, no. 2, pp. 476-481.
- [11] BARBEE, T.W. Jr. et al. *Nano-laminate-based Igniters*. US Patent 8,328,967, 2012.
- [12] RAMOS, A.S. et al. Production of intermetallic compounds from Ti/Al and Ni/Al multilayer thin films – a comparative study. *Journal of Alloys and Compounds*. 2009, vol. 484, no. 1, pp. 335-340.
- [13] NOVÁK, P. et al. Effect of SHS conditions on microstructure of NiTi shape memory alloy. *Intermetallics*. 2013, vol. 42, pp. 85-91.
- [14] NOVÁK, P. et al. Finding the energy source for self-propagating high-temperature production of NiTi shape memory alloy. *Materials Chemistry and Physics*. 2016, vol. 181, pp. 295-300.
- [15] HANUŠ, J. et al. *J. Phys. D: Appl. Phys.* 2017, vol. 50, article 475307.
- [16] PLIMPTON, S. Fast parallel algorithms for short-range molecular dynamics. *Journal of Computational Physics*. 1995, vol. 117, pp. 1-19.
- [17] PASCUET, M. I., FERNANDEZ, J. R. Atomic interaction of the MEAM type for the study of intermetallics in the Al–U alloy. *Journal of Nuclear Materials*. 2015, vol. 467, pp. 229-239.
- [18] HIREL, P. AtomsK: A tool for manipulating and converting atomic data files. *Computer Physics Communications*. 2015, vol. 197, pp. 212-219.
- [19] STUKOWSKI, A. Visualization and analysis of atomistic simulation data with OVITO—the Open Visualization Tool. *Modelling and Simulation in Materials Science and Engineering*. 2009, vol. 18, article 015012.
- [20] BAJTOŠOVÁ, L. et al. Nickel nanoparticles: Insights into sintering dynamics. *Crystals*. 2024, vol. 14, no. 4, article 321. ISSN 2073-4352. DOI: <https://doi.org/10.3390/cryst14040321>.
- [21] TSYGANOV, S. et al. Analysis of Ni nanoparticle gas phase sintering. *Physical Review B*. 2007, vol. 75, article 045421.
- [22] STRAUMAL, P.B. et al. 44Ti self-diffusion in nanocrystalline thin TiO₂ films produced by a low temperature wet chemical process. *Scripta Materialia*. 2018, vol. 149, pp. 31-35. ISSN 1359-6462. DOI: <https://doi.org/10.1016/j.scriptamat.2018.01.022>.
- [23] HOSHINO, K., PETERSON, N.L., WILEY, C.L. Self-diffusion in single crystal and polycrystalline NiO. *Journal of Physics and Chemistry of Solids*. 1985, vol. 46, pp. 1397-1411.